BIOCHEMISTRY
including biophysical chemistry & molecular biology

Article

pubs.acs.org/biochemistry

The Spatial Distribution of Actin and Mechanical Cycle of Myosin Are Different in Right and Left Ventricles of Healthy Mouse Hearts

J. Nagwekar,[†] D. Duggal,[†] R. Rich,[†] S. Raut,[‡] R. Fudala,[†] I. Gryczynski,[†] Z. Gryczynski,[‡] and J. Borejdo*[,†]

[†]Department of Cell Biology and Center for Fluorescence Technology and Nanomedicine, University of North Texas Health Science Center, 3500 Camp Bowie Boulevard, Fort Worth, Texas 76107, United States

[‡]Department of Physics and Astronomy, Texas Christian University, 2800 South University Drive, Fort Worth, Texas 76129, United States

Supporting Information

ABSTRACT: The contraction of the right ventricle (RV) expels blood into the pulmonary circulation, and the contraction of the left ventricle (LV) pumps blood into the systemic circulation through the aorta. The respective afterloads imposed on the LV and RV by aortic and pulmonary artery pressures create very different mechanical requirements for the two ventricles. Indeed, differences have been observed in the contractile performance between left and right ventricular myocytes in dilated cardiomyopathy, in congestive heart failure, and in energy usage and speed of contraction at light loads in healthy hearts. In spite of these functional differences, it is commonly believed that the right and left ventricular muscles are identical because there were no differences in stress development, twitch duration, work performance, or power among the RV and LV in dogs. This report shows that on a mesoscopic scale [when only a few molecules are studied (here three to six molecules of actin) in *ex vivo* ventricular myofibrils], the two ventricles in rigor differ in the degree of orientational disorder of actin within in filaments and during contraction in the kinetics of the cross-bridge cycle.

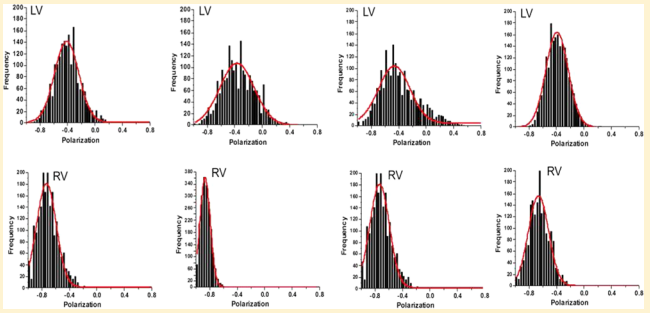

Muscle contraction[1−3] causes a left ventricle of a heart muscle to squeeze blood into an aorta and a right ventricle to squeeze blood into a pulmonary artery. The afterloads imposed by aorta and artery are different, implying that mechanical requirements of the two ventricles should be different. In fact, differences have been observed in the contractile performance between left and right ventricular myocytes in dilated cardiomyopathy[4] and congestive heart failure.[5] Differences were observed in energy usage of healthy LVs and RVs.[6,7] Samarel showed an increased level of fractional synthesis and degradation of myosin heavy chain and light chains, but not actin, in the left compared to the right ventricular free wall.[8] Sordahl[9] observed that mitochondria isolated from the right ventricles had rates of phosphorylation of respiration lower than those of left ventricular mitochondria. The proteomic differences between LVs and RVs have recently been observed.[10] However, Wikman-Coffelt and her collaborators[11] found no differences in stress development, twitch duration, work performance, or power among LVs and RVs in dogs. The two ventricular muscles are morphologically identical. To the best of our knowledge, the issue of mechanical differences between LV and RV muscles has not been resolved.

This report shows that on a mesoscopic scale (when only a few molecules are studied) the two ventricular muscles are different. Specifically, the probability distribution of spatial orientations of actin in the thin filaments, as well as the cross-bridge cycle, is different in LVs and RVs. We were motivated to study a few molecules by the fact that the mean values of a sufficiently large number of independent random measurements, each with a well-defined expected value and well-defined variance, will be approximately normally distributed.[12] Therefore, when whole ventricles are studied, containing at least 10^{18} molecules of actin or myosin (the left ventricle of a B6 mouse typically weighs 30 mg), there is no hope of observing differences between distributions of molecules within ventricles. With regard to kinetics, an argument that a small number of molecules must be studied can also be made. Force-generating molecules are unsynchronized, and macroscopic measurements generate only the average values. The process of averaging large assemblies removes individual contributions, and information about the kinetics is lost.[13,14] In contrast, when only a few molecules are studied, the value of a variable is affected by fluctuations around the average.[15] Fluctuations are caused by chemical reaction,[16] and when the number of observed molecules is small, fluctuations can be very large. The relative size of fluctuations depends on the number of molecules under observation N as $\sqrt{N}/N$. In our experiments, there were typically three to six molecules, and the corresponding

Received: September 18, 2014
Revised: October 29, 2014
Published: November 6, 2014

   dx.doi.org/10.1021/bi501175s | *Biochemistry* 2014, 53, 7641−7649

fluctuations were ∼5−41%. In contrast, if we are dealing with an N on the order of 10^{18} molecules of actin or myosin, the relative fluctuation of a signal is only 0.0000001%, much too small to be detected.

Actin molecules in thin filaments were significantly less well ordered in rigor LVs than RVs. Kinetic analysis revealed that cross-bridges from RVs as compared to LVs displayed a 2-fold decrease in the rate of execution of a power stroke and a 36% decrease in the rate of dissociation from thin filaments. The fact that an increase in macroscopic tension has not been observed earlier suggests that two effects cancel each other. We speculate that the differences between ventricles arise because of the variation of external load between LVs and RVs.

MATERIALS AND METHODS

Chemicals and Solutions. All chemicals were from Sigma-Aldrich (St. Louis, MO). Alexa633-labeled phalloidin (AP) and unlabeled phalloidin (UP) were from Molecular Probes (Eugene, OR). The chemical skinning solution contained 50% glycerol, 1% Triton X-100, 10^{-8} M Ca^{2+}, 3.5 mM free Mg^{2+}, 7 mM EGTA, 2.5 mM Mg-ATP^{2-}, 20 mM Tris (pH 7.0), 15 mM creatine phosphate, and 15 units/mL phosphocreatine kinase. The contracting solution contained 50 mM KCl, 10 mM Tris-HCl (pH 7.5), 5 mM $MgCl_2$, 0.1 mM $CaCl_2$, 5 mM ATP, 20 mM creatine phosphate, and 10 units of 1 mg/mL creatine kinase/mL. The relaxing solution was the same as the contracting solution, but Ca^{2+} was replaced with 2 mM EGTA. The Ca rigor solution contained 50 mM KCl, 10 mM Tris-HCl (pH 7.5), 2 mM $MgCl_2$, and 0.1 mM $CaCl_2$.

Preparation of Ventricles. Whole hearts of healthy 6-month-old female C57BL/6 mice were stored for a few weeks at −80 °C [gift of N. Sumien, Department of Pharmacology, University of North Texas Health Science Center (UNTHSC); fresh hearts were provided by R. Berg, Department of Cell Biology and Immunology, UNTHSC]. Hearts were washed with a cold dissecting solution (50 mM KCl, 5 mM MgEGTA, and 15% glycerol) to wash out ATP without causing contraction. Right and left ventricles were dissected in the dissecting solution in the cold room. They were then chemically skinned by being placed in a skinning solution [15% glycerol, 3.5 mM $MgCl_2$, 20 mM Tris (pH 7.0), 1% Triton X-100, 7 mM EGTA, 2.5 mM ATP, 15 mM creatine phosphate, and 15 units/mL phosphocreatine kinase] for 24 h at 4 °C. After Triton had been washed out, they were either used immediately or stored for up to 3 weeks at −80 °C.

Preparation of Myofibrils. Ventricles were washed three times for 0.5 h with an ice-cold EDTA rigor solution [50 mM KCl, 10 mM Tris-HCl (pH 7.5), and 5 mM EDTA] for 30 min to wash out ATP present in the skinning solution without causing contraction. They were then washed thoroughly with the Ca rigor solution and homogenized in the Cole-Palmer LabGen 125 homogenizer for 10 s followed by homogenization for a further 10 s after a cooling period of 30 s.

Cross-Linking. To inhibit shortening, 1 mg/mL myofibrils were incubated for 20 min at room temperature with 20 mM water-soluble cross-linker 1-ethyl-3-[3-(dimethylamino)-propyl]carbodiimide (EDC).[17−20] The reaction was stopped by adding 20 mM DTT. The pH of the solution remained unchanged at 7.5 throughout the time course of reaction. The absence of shortening was verified by observing myofibrils irrigated with the contraction solution in a Nomarski microscope.

Labeling of Thin Filaments. AP (10 nM) was mixed with 10 μM UP and the mixture added to 1 mg/mL myofibrils for 10 min at room temperature. Figure 1S of the Supporting Information shows a typical image of a ventricular myofibril. Phalloidin is known to impose a higher stiffness[21] on thin filaments but does not alter their function.[22,23]

Number of Observed Myosin Molecules. To determine the number of Alexa-labeled phalloidin molecules under observation, the instrument was calibrated to determine the fluorescence intensity caused by a known number of molecules of Alexa-labeled phalloidin. This number was determined by fluorescence correlation spectroscopy (FCS). At delay time zero, the autocorrelation function (ACF) of fluctuations caused by diffusion of free AP is equal to the inverse of the number of molecules contributing to the fluctuations [$N = 1/\mathrm{ACF}(0)$].[16,24,25] A calibration was made by plotting the number of AP molecules versus the rate of photon arrival. It indicated that the number of photons collected in a second from a single Alexa633-labeled phalloidin molecule illuminated with ∼1 μW of laser power was 1200. An example of the fluorescent signal is shown in Figure 2S of the Supporting Information. Typically, there were three to six molecules in the observational volume (OV). The OV (1.7 μm^3) was estimated by measuring the fwhm of axial and lateral dimensions of an image of 20 nm fluorescent beads and then making a three-dimensional (3D) Gaussian approximation[26] However, it must be emphasized that as long as the number of molecules is mesoscopic, the exact number does not matter; i.e., three molecules should give the same result as 30 molecules, etc.

Each experiment lasted 20 s and included 2 million experimental data points. Because a characteristic lifetime of one fluctuation is on the order of milliseconds,[27] each data set was binned (smoothed) to contain 20000 fluctuations. If X is the number of fluctuations detected, the precision of the measurement is approximately equal to $1/\sqrt{X}$. Hence, the precision of our experiment is ∼0.5%.

Time-Resolved Anisotropy Measurements. To ascertain whether the phalloidin probe is immobilized so that the transition dipole of the fluorophore reflects the orientation of the protein, we measured the decay of anisotropy of AP inserted into myofibrils. Anisotropy is defined as $r = (I_{\parallel} - I_{\perp})/(I_{\parallel} + 2I_{\perp})$. The fluorescence anisotropy was measured by the time domain technique using a FluoTime 200 fluorometer (PicoQuant, Inc.) at room temperature. The excitation was provided by a 635 nm pulsed diode laser, and the observation was conducted through a 670 nm monochromator with a supporting 650 nm long pass filter. The full width at half-maximum (fwhm) of the pulse response function was <100 ps, and the time resolution was <10 ps. The intensity decays were analyzed by a multiexponential model using FluoFit (PicoQuant, Inc.).

Data Collection. The myofibrils were placed on a scanning stage of a PicoQuant MT 200 inverse time-resolved fluorescence instrument coupled to an Olympus IX 71 microscope. The stage was rotated to align vertically a myofibril under observation. Before each experiment, the fluorescence of an isotropic solution of a small dye with a long fluorescence lifetime (rhodamine 700, which has zero anisotropy) was measured to make sure that the parallel (∥) and perpendicular (⊥) channels received an equal amount of emitted light. A 640 nm laser beam modulated at 20 MHz was focused by an Olympus 60×, NA 1.2 water immersion objective to the diffraction limit on the fluorescent part of a myofibril. The

dx.doi.org/10.1021/bi501175s | Biochemistry 2014, 53, 7641−7649

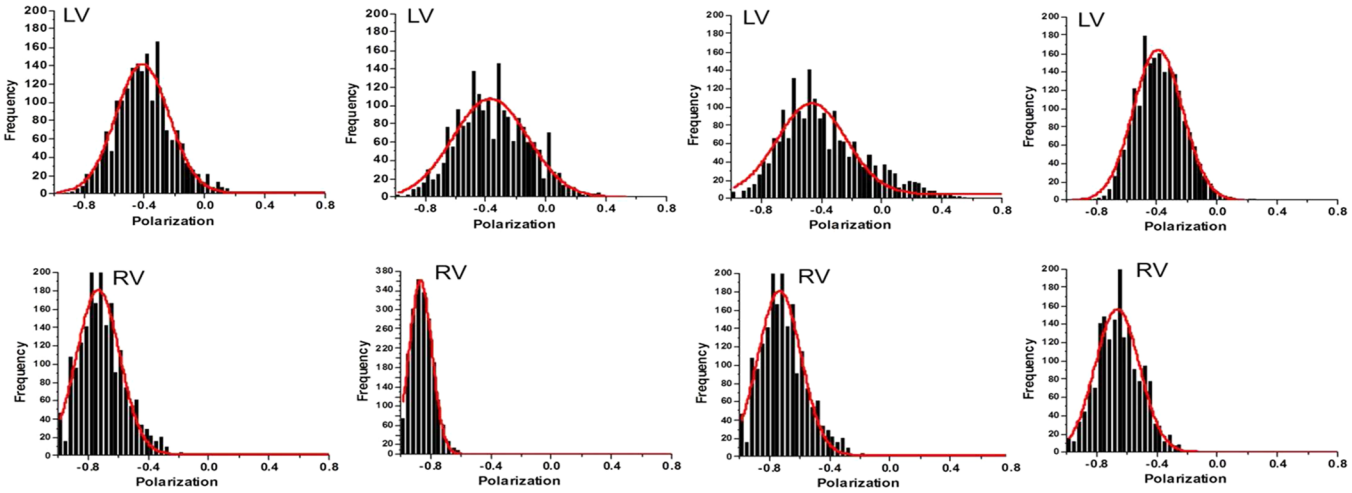

Figure 1. Examples of distributions of polarization values of actin transition dipoles in rigor.

power delivered to each half-sarcomere was adjusted within a range of 1−2 μW to obtain a similar photon rate for each myofibril. If the power is not equal, the differences between data sets become statistically interpretable; ∼25−50 myofibrils were examined. We measured the polarization of fluorescence (PF) rather than steady-state anisotropy (R). The PF is the normalized ratio of the difference between ∥ and ⊥ components of the fluorescent light emitted by the dye. The relation between the two is PF = $R/(2 + R)$. Dos Remedios, Morales, and others have shown that PF is a sensitive indicator of the conformation of the transition dipole of the fluorophore.[2,3,28−32]

Statistical Analysis. The rate constants were measured from the slope of the autocorrelation function. A typical ACF was a single rectangular hyperbola that was linearized as shown in Figure 3S of the Supporting Information. The slope was determined by the best square fit by Origin (version 8.6, OriginLab Corp., Northampton, MA). Comparisons between groups were performed using an unpaired Student's t test (Sigma Plot 11, Systat Software, Inc., San Jose, CA). The differences were deemed significant when $P < 0.05$. SigmaPlot 11 was used to compute histograms. Origin was used to compute autocorrelation functions.

RESULTS

Distribution of Actin Orientations. Experiments were conducted in rigor. Rigor XBs are rigidly attached to actin monomers. Therefore, their fluorescence transition dipoles are mostly immobilized, and their steady-state anisotropy (SSA) values are high (Figure 4b). Deviations of polarization values from the mean arise from the fact that not all rigor bonds are precisely the same.

The probability distribution of polarized fluorescence data is best represented in the form of a histogram, a plot of polarization versus probability of it occurring within a given experiment. Examples of histograms of the experiments on LVs and RVs are shown in the top and bottom panels, respectively, of Figure 1. The degree of actin disorder is best expressed by the value of the full width at half-maximum of a histogram (fwhm). It measures the width of the distribution at the point where the maximal probability is the largest.[a] All data are summarized in Table 1.

Table 1. Widths of Angular Distributions of Actin Transition Dipoles in Rigor LVs and RVs[a]

	fwhm	polarization	counts/ms
LV	0.438 ± 0.069	−0.416 ± 0.057	8.756 ± 2.774
RV	0.339 ± 0.144	−0.762 ± 0.276	6.171 ± 2.029

[a]The results are averages of 25 experiments on different LVs and RVs. Errors are standard deviations.

fwhm values of actins of RVs were significantly narrower (better ordered) than those of LVs. The difference between LVs and RVs is statistically significant (two-tailed $t = 2.986$; $P = 0.004$, with 42 degrees of freedom). The 95% confidence interval of this difference ranged from 0.03210 to 0.16590. The difference in the polarization values was extremely statistically significant (the two-tailed P value is <0.0001 with 42 degrees of freedom). The 95% confidence interval of this difference ranged from 0.22968 to 0.46232. The difference in counts per millisecond (fluorescence intensity) was statistically insignificant.

We report the fluorescence intensity of the signal because in static experiments it is crucial that the mean fluorescence intensity be taken into account. This is because the fwhm of the Gaussian distribution of polarizations depends not only on the properties of muscle but also on the strength of the signal. Strong Gaussian signals give small fwhms, and weak signals give large fwhms. Importantly, in our experiments, the difference between intensities of LV and RV signals was insignificant.

Another way to characterize differences between LVs and RVs is to measure their skewness and kurtosis (Table 2). Skewness is a measure of the lack of symmetry of a distribution. The skewness of an ideal Gaussian distribution is 0. Kurtosis is a measure of whether the data are peaked or flat relative to the normal distribution. High-kurtosis histograms have a distinct

Table 2. Skewness and Kurtosis of the Distribution of Actin Orientations[a]

	skewness	excess kurtosis
rigor LV	1.141 ± 0.172	0.785 ± 0.467
rigor RV	2.187 ± 0.655	3.599 ± 2.491

[a]From 25 experiments on different LVs and RVs. Errors are standard deviations.

dx.doi.org/10.1021/bi501175s | *Biochemistry* 2014, 53, 7641−7649

Table 3. Widths of Angular Distributions of Actin Transition Dipoles in Relaxed LVs and RVs[a]

	fwhm	counts/ms	polarization	skewness	kurtosis
LV	0.414 ± 0.075	6.476 ± 1.849	−0.631 ± 0.223	1.743 ± 0.567	2.256 ± 2.575
RV	0.416 ± 0.266	6.791 ± 1.923	−0.822 ± 0.698	1.790 ± 0.571	2.344 ± 3.435

[a]The results are averages of 22 experiments with different LVs and RVs. Errors are standard deviations.

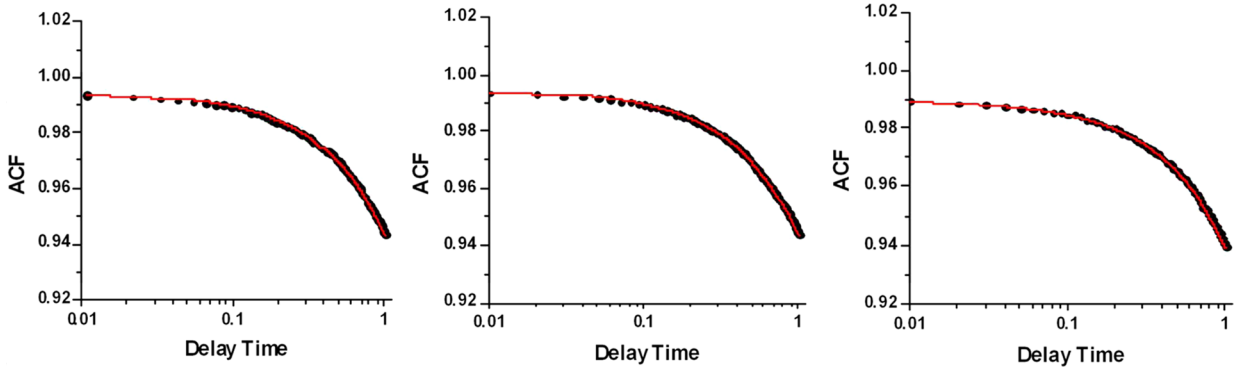

Figure 2. Examples of ACFs of contracting ventricular myofibrils. The decays were fit (red line) by a model shown in Figure 4. This model allows calculation of the rate of the power stroke (k_2) and the rate of dissociation of XBs from thin filaments (k_3). Red lines are the best fits from the model of Mettikola et al.,[35] reproduced here in Figure 5S of the Supporting Information. This model includes the rate of binding of XB to thin filaments (k_1), but we were not able to resolve; it is probably too rapid. We present only averages of rates k_2 and k_3. The horizontal axes are on a logarithmic scale. Figure 3S of the Supporting Information explains how the rate constants are calculated after converting a log scale to a linear scale.

Table 4. Mean Values and Standard Deviations of Rate Constants from 27 Experiments

contracting ventricle	k_2 (s^{-1})	k_3 (s^{-1})	AR^2 for k_2	AR^2 for k_3
LV	0.159 ± 0.086	0.061 ± 0.026	0.639 ± 0.236	0.920 ± 0.103
RV	0.085 ± 0.035	0.0492 ± 0.008	0.629 ± 0.188	0.972 ± 0.022

peak near the mean. Conversely, low-kurtosis histograms have a flat top near the mean rather than a sharp peak. The kurtosis of an ideal Gaussian distribution is 0.

The difference in skewness was extremely statistically significant (t = 5.589; P < 0.0001, with 42 degrees of freedom). The 95% confidence interval of this difference ranges from −1.05619 to −0.49581. The difference in kurtosis was also extremely statistically significant (t = 5.501; P < 0.0001, with 42 degrees of freedom). The 95% confidence interval for the difference in means ranges from −4.233 to −1.959.

The fact that kurtosis of rigor distributions of RV muscles is high suggests that XBs bind to actin predominantly in a single orientation; i.e., binding is stereospecific. This seems not to be the case in LVs. The point is further argued in the Discussion.

Relaxation as a Negative Control. During relaxation, XBs do not make contact with actin filaments, which results in a disorder.[33,34] We expected histograms of the polarization of fluorescence of actin to be the same for both ventricles. This was indeed the case. The examples of distributions of actin in relaxation are shown in Figure 4S of the Supporting Information. Data are summarized in Table 3.

None of the differences were statistically significant. The −0.00216 difference in fwhm was *not* statistically significant (t = −0.0359; P = 0.971, with 42 degrees of freedom). The 95% confidence interval for the difference in means ranges from −0.124 to 0.119. The −0.315 difference in the rate of photon arrival was *not* statistically significant (t = −0.552; P = 0.584, with 42 degrees of freedom). The 95% confidence interval for the difference in means ranges from −1.465 to 0.835. The 0.191 difference in polarization was *not* statistically significant (t = 1.198; P = 0.237, with 42 degrees of freedom). The 95% confidence interval for the difference in means ranges from −0.131 to 0.513. The −0.0463 difference in skewness was *not* statistically significant (t = −0.269; P = 0.789, with 42 degrees of freedom). The 95% confidence interval for the difference in means ranges from −0.393 to 0.300. The −0.0888 difference in kurtosis was *not* statistically significant (t = −0.0963; P = 0.924, with 42 degrees of freedom). The 95% confidence interval for the difference in means ranges from −1.950 to 1.773.

Kinetics. Kinetics is extracted from the analysis of fluctuations.[13,16] The fluctuations occur because the transition dipole of actin changes during contraction, with myosin XBs constantly binding to and dissociating from the thin filaments. While most of these interactions have no effect on polarization (because only 1 in 1000 actin monomers is fluorescent), sometimes they do have an effect (explained in more detail in Figure 3). Figure 4 explains why the fluctations of the transition dipoles of the few labeled actin molecules provide insight into the mechanical cycle of XBs. Figure 2 shows representative examples of autocorrelation functions of myofibrils from a typical ventricle.

The results of fits to 27 experiments are summarized in Table 4. A good measure of the goodness of fit is adjusted R^2 (AR^2) because it accounts for the number of degrees of freedom. The best fit gives a value of 1. The AR^2 for the ACF fit was significantly better for the average value of k_3 than that of k_2 (t = 4.086; P < 0.001, with 41 degrees of freedom).

The difference in k_2 between LVs and RVs was highly statistically significant (t = 4.275; P < 0.001, with 46 degrees of freedom). The 95% confidence interval for the difference in means ranges from 0.123 to 0.0441. The difference in k_3 was statistically significant (t = −2.239; P = 0.030, with 51 degrees

dx.doi.org/10.1021/bi501175s | *Biochemistry* 2014, 53, 7641−7649

of freedom). The 95% confidence interval for the difference in means ranges from 0.0346 to 0.00189.

DISCUSSION

Distribution of Actin Orientations. This report shows that on a mesoscopic scale the spatial distribution of actin monomers (and therefore the degree of order) within thin filaments in LVs and RVs is different. However, because there have been no confirmed reports of any amino acid or conformational differences in LVs and RVs of myosin heavy or light chains, it is commonly believed that the right and left ventricular muscles responsible for contraction are identical, yet the afterloads imposed on the LV and RV by aortic and pulmonary artery pressures cause different mechanical requirements of the two ventricles. As mentioned above, the whole ventricles contain at least 10^{18} molecules of actin or myosin. If one makes a sufficiently large number of independent random measurements, each with a well-defined expected value and well-defined variance, the distribution will be approximately normal.[12] Therefore, when whole ventricles are studied, there is no hope of observing differences between distributions of polarization of fluorescence (or any other property) of molecules within ventricles. Via the limitation of the number of observed molecules in *ex vivo* ventricles, it was possible to detect differences in the degree of order. The fwhm (of polarized fluorescence or any other property of observed molecules) can be significantly affected only when an individual molecule makes a substantial contribution to the overall signal. When the number is small, the orientations that are the most likely to appear first are the most probable. Less probable ones (those contained in the outliers of distributions) are less likely to appear. As a consequence, the histograms of a distribution of a few molecules are mostly populated by the most likely orientations, lacking the outliers of the distribution. The lack of outliers magnifies the differences in fwhms. The fact that kurtosis of rigor distributions of the RV is high indicates that the data are peaked relative to the normal distribution. This implies that there is a well-defined orientation of the transition dipole of actin and therefore of XB that affects this monomer and suggests that the binding of XBs to actin in RV is stereospecific.

Kinetics. There are three requirements for making kinetic measurements. First, the data must be obtained *ex vivo*, not from isolated molecules *in vitro*. An ensemble of myosin molecules in muscle cannot be viewed as a collection of independent motors because individual motors interact mechanically by accelerating ADP release and increasing the reach of the XBs when attached.[36] Second, it must be recognized that in contracting muscle the force-generating molecules act in an unsynchronized fashion. Thus, to obtain kinetic information, the molecules have to be synchronized by applying transients[2737] or white noise.[38] The alternative is to collect data from a small assembly of force generators. We chose this alternative, because the other approaches are difficult to apply *in vivo*. Measurements from large assemblies are averages, containing no kinetic information from all molecules. In contrast, the average of a small assembly does contain kinetic information in the form of large fluctuations from the average.[13,14] Third, *ex vivo* information must be obtained with a millisecond time resolution, because XBs are expected to rotate rapidly.[27] Super-resolution microscopy using single molecules *in vivo* is a conceivable method but has a limited time resolution.[b] We have achieved the necessary time resolution by sampling a small volume of muscle containing only a few labeled molecules.

We now explain why observing the orientation of actin dipoles provides information about the kinetics of a XB. As mentioned above, the polarized fluorescence of the transition dipole of actin fluctuates because myosin XBs are constantly binding to and dissociating from actin. While most of these interactions have no effect on polarization (because only 1 in 1000 actin monomers is fluorescent), sometimes they do have an effect. This is illustrated in Figure 3. Fourteen actin monomers are connected by the tropomyosin double helix that acts as a cooperative unit.[44−49] Each interaction of the myosin head (mostly with the unlabeled actin) results in no change in the dipole orientation of labeled actin (e.g., XBs 2 and 3) because it occurs too far from the labeled actin monomer, but the few XBs that bind within the cooperative unit (e.g., XB 1) will cause a change in the orientation of the actin dipole.

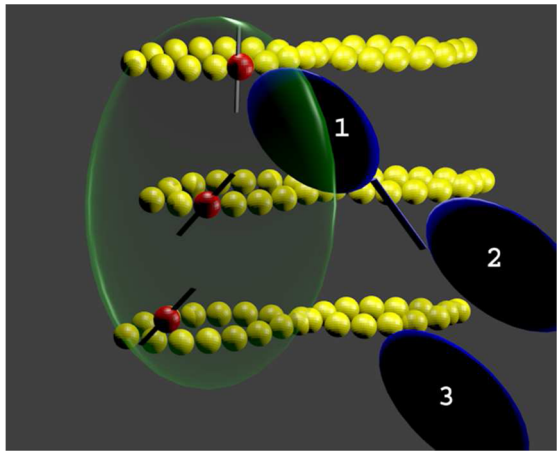

Figure 3. Sparse labeling of myofibrils. Thin filaments are irrigated with a 0.1% mixture of Alexa633-labeled phalloidin and unlabeled phalloidin. As a result, only 1 in 1000 actins is labeled (red) and 999 are not (yellow). The dipole moment of rhodamine is indicated by the black line. Only XB 1 affects the direction of the actin dipole. The myofibril is illuminated with 640 nm light. The detector sees only the volume equivalent to the transparent green ellipsoid of revolution (not drawn to scale).

The changes in those dipole moments that are affected by interactions with myosin heads do reflect the XB cycle (remembering that labeled actins that are too far from the interacting myosin head and unlabeled actins do not contribute to the change in signal). The basic cycle is shown in Figure 4. In this scheme, based on models of Lymn and Taylor,[50] Coureux, Sweeney, and Houdusse,[51] and Spudich,[52] starting from panel c, the myosin head (blue) containing products of hydrolysis is not attached to the thin filament and rotates nearly freely in the myofilament space as does the transition dipole of Alexa633-labeled phalloidin (green arrow). The closest labeled actin protomer (red sphere) also rotates rapidly because it is not restrained by a XB. Its steady-state anisotropy (SSA) is small (0.041, inset in panel c). In the next step (panel a), myosin binds to actin with a rate k_1. At the same time, the SSA of actin increases to 0.180 (inset of panel a). The next step (panel b) involves the release of phosphate and ADP (not necessarily in that order), during which a XB executes a power stroke with a rate constant k_2 to bind strongly to actin. Actin rotation now becomes restricted [SSA = 0.265 (inset of panel

dx.doi.org/10.1021/bi501175s | *Biochemistry* 2014, 53, 7641−7649

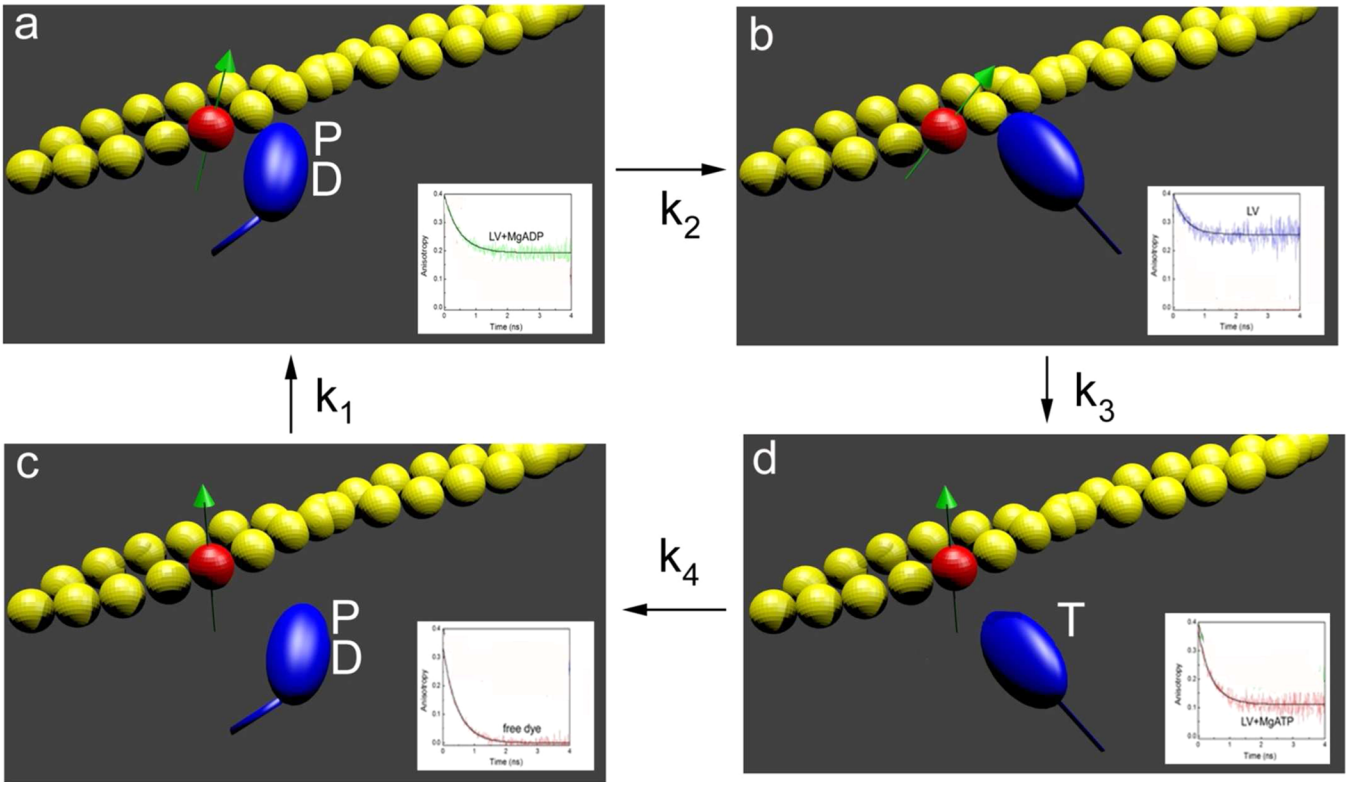

Figure 4. Conventional model of XB action showing that the steady-state orientation of labeled actin [red sphere; the orientation of phalloidin (its fluorescent transition dipole) is indicated by a green arrow] is different in different intermediate states (0.1 mg/mL myofibrils labeled with 0.01 μM AP and 10 μM UP). ATP is T, ADP D, and P_i P.

b)]. This is followed by XB binding of a fresh molecule of ATP and dissociation of myosin from actin at a rate k_3. Actin rotation now becomes more free [SSA = 0.133 (inset of panel d)]. It is a pseudo-first-order reaction because the concentration of ATP is much greater than the myosin concentration (i.e., the ATP concentration is constant). Hydrolysis of ATP with a rate k_4 reverses the power stroke and reprimes the head. This conformational change is not recorded.

Observing Actin Rather Than Myosin XBs. This approach has several important advantages. First, in mesoscopic measurements, it is crucial to be able to label a small number of molecules and to know precisely how many molecules are labeled. Irrigating myofibrils with the exact ratio of labeled and unlabeled phalloidin allows one to accomplish this. Second, it avoids measuring the rate of repriming (back stroke). Omitting it considerably simplifies the analysis. An autocorrelation function of the four-state cycle is very complex,[53] whereas the three-state cycle proved to be manageable.[35] Third, labeling of actin with phalloidin is very reproducible[54] because labeling of actin involves only gentle irrigation of myofibrils with the protein at room temperature, whereas direct labeling of myosin involves labeling light chain 1 (LC1) and exchanging it with myofibrillar LC1 under harsh conditions (0.5 h at 37 °C in the presence of trifluoroperazine).[55] However, there are disadvantages of labeling actin. Labeling myosin directly with bifunctional rhodamine is well-understood.[19,56] Part of a XB that undergoes the most prominent rotation, its regulatory light chain, is probed directly, and in contrast to XB labeled with Alexa633-labeled phalloidin, the dipole moment of bifunctional rhodamine in rigor is 100% immobilized by thin filaments.

CONCLUSIONS

Summarizing Data about the Distribution of Actin Orientations. Statistical analysis of rigor muscle revealed that all static parameters were different in rigor LVs and RVs. In particular, the fwhm of RV muscle was significantly smaller than that of LV muscle. This may reflect the stereospecific character of rigor bond in the RV.

Summarizing Kinetic Data. The rate of power stroke (k_2) of XBs was significantly higher in the LV than in the RV. This would have led to the development of more tension. The rate of dissociation from the thin filament (k_3) was also significantly higher in LV muscle. Faster dissociation would have led to the development of less tension, because XBs would spend less time in the tension-generating state. The fact that an increase in macroscopic tension has not been observed suggests that two effects offset each other. Myosin molecules from left and right ventricular muscles may be different as a result of differences in force requirements that could lead to epigenetic changes in DNA. One possible mechanism is histone deacetylation followed by oxidation and phosphorylation, to cause histone deacetylases (HDACs) to exit the nucleus and cause observed differences between ventricles. It is conceivable that this hypothesis could be tested by knocking out genes encoding HDACs.

The detection of a few myosin molecules in an *ex vivo* ventricle with a millisecond time resolution is not technically easy. The main problem is that the signals are weak. Weak Gaussian signals with a low signal-to-noise ratio have an intrinsically large relative error. This also applies to the ratio of these signals, as shown by Midde et al.[57] It is thus remarkable that we were able to measure the fwhm and kinetic constant

dx.doi.org/10.1021/bi501175s | *Biochemistry* 2014, 53, 7641−7649

with relatively high accuracy, in spite of the nonuniform incorporation of AP into sarcomeres (Figure 1S of the Supporting Information), differing degrees of phosphorylation of myofibrils,[58] a relatively low steady-state anisotropy of AP, and consequently relatively small differences in anisotropy between different mechanochemical steps. The photobleaching and light scattering from a sample add to the degree of error of the results.

More work is required to address the issues mentioned above and to determine whether the observed differences between the XBs of mouse left and right ventricles are characteristic of all mammalian muscles or whether they are specific for the hearts of small rodents. Further, it should be mentioned that phosphorylation levels of myosin binding protein C (MBP-C) may influence the distribution and kinetics of XBs in ventricles. MBP-C binds to both actin and myosin heads through the N-terminus.[59] It is believed to stabilize the binding of the myosin head to the core of the thick filament. Any of the three sites for phosphorylation of cardiac MBP-C can be phosphorylated by a variety of kinases. Phosphorylation at some of these sites causes myosin heads to be released from the core of the thick filament and become disordered. It is possible that protein C acts as a signaling molecule, reporting changes in cross-bridges to actin. Indeed, recent data suggest that MyBP-C may alter the interaction between cross-bridges and actin.[60]

■ ASSOCIATED CONTENT

Supporting Information

Figures 1S−5S. This material is available free of charge via the Internet at http://pubs.acs.org.

■ AUTHOR INFORMATION

Corresponding Author

*Department of Cell Biology and Immunology, University of North Texas Health Science Center, 3500 Camp Bowie Blvd., Fort Worth, TX 76107. E-mail: julian.borejdo@unthsc.edu. Telephone: (817) 735-2106. Fax: (817) 735-2118.

Author Contributions

This work was supported, in whole or in part, by National Institutes of Health Grants R01 HL071778, R01 AR048622 (to J.B.) ,and R01HL090786 (to J.B. and Dr. D. Szczesna-Cordary).

Notes

The authors declare no competing financial interest.

■ ACKNOWLEDGMENTS

We thank Dr. Nathalie Sumien, Dr. Rance Berg, and Dr. Irina Akopova for supplying and dissecting mouse hearts.

■ ABBREVIATIONS

ACF, autocorrelation function; AP, Alexa633-labeled phalloidin; EDC, ethyl-3-[3-(dimethylamino)propyl]carbodiimide; FCS, fluorescence correlation spectroscopy; fwhm, full width at half-maximum; LV, left ventricle; OV, observational volume; PF, polarization of fluorescence; RV, right ventricle; SD, standard deviation; UP, unlabeled phalloidin; XB, myosin cross-bridge.

■ ADDITIONAL NOTES

[a]If the distributions were perfectly normal, fwhm would equal $2(2 \ln 2)^{1/2} = 2.355$ SD (standard deviation).

[b]Achieving such a time resolution is impossible using super-resolution microscopes.[39−41] The unsurpassed spatial resolution of these microscopes is achieved at the expense of time resolution. Even structured illumination, using a sCMOS cameras such as a DeltaVision OMX instrument,[42] needs 2 s to image a single slice of a 3D stack. Rapid super-resolution imaging in live cells can be achieved by analog image processing,[43] but it is unlikely that they can reach the millisecond time resolution required to follow the conformational changes of myosin XBs.

■ REFERENCES

(1) Geeves, M. A., and Holmes, K. C. (2005) The molecular mechanism of muscle contraction. *Adv. Protein Chem. 71* (24), 161−193.

(2) Sabido-David, C., Brandmeier, B., Craik, J. S., Corrie, J. E., Trentham, D. R., and Irving, M. (1998) Steady-state fluorescence polarization studies of the orientation of myosin regulatory light chains in single skeletal muscle fibers using pure isomers of iodoacetamidotetramethylrhodamine. *Biophys. J. 74* (6), 3083−3092.

(3) Hopkins, S. C., Sabido-David, C., van der Heide, U. A., Ferguson, R. E., Brandmeier, B. D., Dale, R. E., Kendrick-Jones, J., Corrie, J. E., Trentham, D. R., Irving, M., and Goldman, Y. E. (2002) Orientation changes of the myosin light chain domain during filament sliding in active and rigor muscle. *J. Mol. Biol. 318* (5), 1275−1291.

(4) McMahon, W. S., Mukherjee, R., Gillette, P. C., Crawford, F. A., and Spinale, F. G. (1996) Right and left ventricular geometry and myocyte contractile processes with dilated cardiomyopathy: Myocyte growth and β-adrenergic responsiveness. *Cardiovasc. Res. 31* (2), 314−323.

(5) Belin, R. J., Sumandea, M. P., Sievert, G. A., Harvey, L. A., Geenen, D. L., Solaro, R. J., and de Tombe, P. P. (2011) Interventricular differences in myofilament function in experimental congestive heart failure. *Pfluegers Arch. 462* (6), 795−809.

(6) Carlsson, M., Heiberg, E., Toger, J., and Arheden, H. (2012) Quantification of left and right ventricular kinetic energy using four-dimensional intracardiac magnetic resonance imaging flow measurements. *Am. J. Physiol. 302* (4), H893−H900.

(7) Itoya, M., Mallet, R. T., Gao, Z. P., Williams, A. G., Jr., and Downey, H. F. (1996) Stability of high-energy phosphates in right ventricle: Myocardial energetics during right coronary hypotension. *Am. J. Physiol. 271* (1, Part 2), H320−H328.

(8) Samarel, A. M. (1989) Regional differences in the in vivo synthesis and degradation of myosin subunits in rabbit ventricular myocardium. *Circ. Res. 64* (2), 193−202.

(9) Sordahl, L. A. (1976) Differences in mitochondrial functions from right and left ventricular myocardium of four mamalian species. *Comp. Biochem. Physiol. 54B*, 339−342.

(10) Cadete, V. J., Lin, H. B., Sawicka, J., Wozniak, M., and Sawicki, G. (2012) Proteomic analysis of right and left cardiac ventricles under aerobic conditions and after ischemia/reperfusion. *Proteomics 12* (14), 2366−2377.

(11) Wikman-Coffelt, J., Fenner, C., Smith, A., and Mason, D. T. (1975) Comparative analyses of the kinetics and subunits of myosins from canine skeletal muscle and cardiac tissue. *J. Biol. Chem. 250* (4), 1257−1262.

(12) Rice, J. (1995) *Mathematical Statistics and Data Analysis*, 2nd ed., Duxbury Press, Pacific Grove, CA.

(13) Elson, E. L., and Magde, D. (1974) Fluorescence Correlation Spectroscopy: Coceptual Basis and Theory. *Biopolymers 13*, 1−28.

(14) Elson, E. L., and Webb, W. W. (1975) Concentration correlation spectroscopy: A new biophysical probe based on occupation number fluctuations. *Annu. Rev. Biophys. Bioeng. 4*, 311−334.

(15) Qian, H., Saffarian, S., and Elson, E. L. (2002) Concentration fluctuations in a mesoscopic oscillating chemical reaction system. *Proc. Natl. Acad. Sci. U.S.A. 99* (16), 10376−10381.

(16) Magde, D., Elson, E. L., and Webb, W. W. (1974) Fluorescence correlation spectroscopy. II. An experimental realization. *Biopolymers 13* (1), 29−61.
(17) Herrmann, C., Lionne, C., Travers, F., and Barman, T. (1994) Correlation of ActoS1, myofibrillar, and muscle fiber ATPases. *Biochemistry 33* (14), 4148−4154.
(18) Tsaturyan, A. K., Bershitsky, S. Y., Burns, R., and Ferenczi, M. A. (1999) Structural changes in the actin-myosin cross-bridges associated with force generation induced by temperature jump in permeabilized frog muscle fibers. *Biophys. J. 77* (1), 354−372.
(19) Bershitsky, S. Y., Tsaturyan, A. K., Bershitskaya, O. N., Mashanov, G. I., Brown, P., Burns, R., and Ferenczi, M. A. (1997) Muscle force is generated by myosin heads stereospecifically attached to actin. *Nature 388* (6638), 186−190.
(20) Barman, T., Brune, M., Lionne, C., Piroddi, N., Poggesi, C., Stehle, R., Tesi, C., Travers, F., and Webb, M. R. (1998) ATPase and shortening rates in frog fast skeletal myofibrils by time-resolved measurements of protein-bound and free Pi. *Biophys. J. 74* (6), 3120−3130.
(21) Grazi, E., Cintio, O., and Trombetta, G. (2004) On the mechanics of the actin filament: The linear relationship between stiffness and yield strength allows estimation of the yield strength of thin filament in vivo. *J. Muscle Res. Cell Motil. 25* (1), 103−105.
(22) dos Remedios, C. G., and Moens, P. D. J. (1995) Actin and the actomyosin interface: A review. *Biochim. Biophys. Acta 1228*, 99−124.
(23) Miki, M., Barden, J., dos Remedios, C., Philips, L., and Hambly, B. D. (1987) Interaction of phalloidin with chemically modified actin. *Eur. J. Biochem. 165*, 125−130.
(24) Elson, E. L. (1985) Fluorescence correlataion spectroscopy and photobleaching recovery. *Annu. Rev. Phys. Chem. 36*, 379−406.
(25) Elson, E. L. (2007) Introduction to FCS. *Short Course on Cellular and Molecular Fluorescence* (Gryczynski, Z., Ed.) Vol. 2, pp 1−10, University of North Texas, Fort Worth, TX.
(26) Buschmann, V., Kramer, B., and Koberling, F. (2009) *Quantitive FCS: Determination of confocal volume by FCS and bead scabnning with Micro Time 200*, PicoQuant, Application Note Quantitative FCS version 1.1.
(27) Huxley, A. F., and Simmons, R. M. (1971) Proposed mechanism of force generation in striated muscle. *Nature 233*, 533−538.
(28) Dos Remedios, C. G., Millikan, R. G., and Morales, M. F. (1972) Polarization of tryptophan fluorescence from single striated muscle fibers. A molecular probe of contractile state. *J. Gen. Physiol. 59*, 103−120.
(29) Nihei, T., Mendelson, R. A., and Botts, J. (1974) Use of fluorescence polarization to observe changes in attitude of S1 moieties in muscle fibers. *Biophys. J. 14*, 236−242.
(30) Tregear, R. T., and Mendelson, R. A. (1975) Polarization from a helix of fluorophores and its relation to that obtained from muscle. *Biophys. J. 15*, 455−467.
(31) Morales, M. F. (1984) Calculation of the polarized fluorescence from a labeled muscle fiber. *Proc. Natl. Acad. Sci. U.S.A. 81*, 145−149.
(32) Hopkins, S. C., Sabido-David, C., Corrie, J. E., Irving, M., and Goldman, Y. E. (1998) Fluorescence polarization transients from rhodamine isomers on the myosin regulatory light chain in skeletal muscle fibers. *Biophys. J. 74* (6), 3093−3110.
(33) Thomas, D. D., and Cooke, R. (1980) Orientation of spin-labeled myosin heads in glycerinated muscle fibers. *Biophys. J. 32* (3), 891−906.
(34) Borejdo, J., Assulin, O., Ando, T., and Putnam, S. (1982) Cross-bridge orientation in skeletal muscle measured by linear dichroism of an extrinsic chromophore. *J. Mol. Biol. 158*, 391−414.
(35) Mettikolla, P., Calander, N., Luchowski, R., Gryczynski, I., Gryczynski, Z., Zhao, J., Szczesna-Cordary, D., and Borejdo, J. (2011) Cross-bridge Kinetics in Myofibrils Containing Familial Hypertrophic Cardiomyopathy R58Q Mutation in the Regulatory Light Chain of Myosin. *J. Theor. Biol. 284*, 71−81.
(36) Walcott, S., Warshaw, D. M., and Debold, E. P. (2012) Mechanical Coupling between Myosin Molecules Causes Differences between Ensemble and Single-Molecule Measurements. *Biophys. J. 103* (3), 501−510.
(37) Dantzig, J. A., Higuchi, H., and Goldman, Y. E. (1998) Studies of molecular motors using caged compounds. *Methods Enzymol. 291*, 307−348.
(38) Kawai, M., and Zhao, Y. (1993) Cross-bridge scheme and force per cross-bridge state in skinned rabbit psoas muscle fibers. *Biophys. J. 65* (2), 638−651.
(39) Hell, S. W., and Wichmann, J. (1994) Breaking the diffraction resolution limit by stimulated emission: Stimulated-emission-depletion fluorescence microscopy. *Opt. Lett. 19*, 780−782.
(40) Shroff, H., White, H., and Betzig, E. (2008) Photoactivated localization microscopy (PALM) of adhesion complexes. *Current Protocols in Cell Biology*, Chapter 4, Unit 4, 21, Wiley, New York.
(41) Heintzmann, R., and Ficz, G. (2013) Breaking the resolution limit in light microscopy. *Methods Cell Biol. 114*, 525−544.
(42) Vision, D. (2013) *OMX* (http://www.api.com/downloads/pdfs/lifescience/DV%20OMX.pdf).
(43) York, A. G., Chandris, P., Nogare, D. D., Head, J., Wawrzusin, P., Fischer, R. S., Chitnis, A., and Shroff, H. (2013) Instant super-resolution imaging in live cells and embryos via analog image processing. *Nat. Methods 10*, 1122−1126.
(44) Yanagida, T., and Oosawa, F. (1978) Polarized fluorescence from ε-ADP incorporated into F-actin in a myosin-free single fiber: Conformation of F-actin and changes induced in it by heavy meromyosin. *J. Mol. Biol. 126* (3), 507−524.
(45) Yanagida, T., and Oosawa, F. (1980) Conformational changes of F-actin-ε-ADP in thin filaments in myosin-free muscle fibers induced by Ca^{2+}. *J. Mol. Biol. 140* (2), 313−320.
(46) Prochniewicz-Nakayama, E., Yanagida, T., and Oosawa, F. (1983) Studies on conformation of F-actin in muscle fibers in the relaxed state, rigor, and during contraction using fluorescent phalloidin. *J. Cell Biol. 97*, 1663−1667.
(47) Oosawa, F., Maeda, Y., Fujime, S., Ishiwata, S., Yanagida, T., and Taniguchi, M. (1977) Dynamic characteristics of F-actin and thin filaments in vivo and in vitro. *J. Mechanochem. Cell Motil. 4* (1), 63−78.
(48) Ando, T. (1989) Propagation of Acto-S-1 ATPase reaction-coupled conformational change in actin along the filament. *J. Biochem. 105* (5), 818−822.
(49) Hill, T. L., Eisenberg, E., and Chalovich, J. M. (1981) Theoretical models for cooperative steady-state ATPase activity of myosin subfragment-1 on regulated actin. *Biophys. J. 35* (1), 99−112.
(50) Lymn, R. W., and Taylor, E. W. (1971) Mechanism of adenosine triphosphate hydrolysis by actomyosin. *Biochemistry 10*, 4617−4624.
(51) Coureux, P. D., Sweeney, H. L., and Houdusse, A. (2004) Three myosin V structures delineate essential features of chemo-mechanical transduction. *EMBO J. 23* (23), 4527−4537.
(52) Spudich, J. A. (2014) Hypertrophic and Dilated Cardiomyopathy: Four Decades of Basic Research on Muscle Lead to Potential Therapeutic Approaches to These Devastating Genetic Diseases. *Biophys. J. 106* (3), 1236−1249.
(53) Mettikolla, P., Calander, N., Luchowski, R., Gryczynski, I., Gryczynski, Z., and Borejdo, J. (2010) Observing cycling of a few cross-bridges during isometric contraction of skeletal muscle. *Cytoskeleton 67* (6), 400−411.
(54) Borejdo, J., Shepard, A., Dumka, D., Akopova, I., Talent, J., Malka, A., and Burghardt, T. P. (2004) Changes in orientation of actin during contraction of muscle. *Biophys. J. 86*, 2308−2317.
(55) Ling, N., Shrimpton, C., Sleep, J., Kendrick-Jones, J., and Irving, M. (1996) Fluorescent probes of the orientation of myosin regulatory light chains in relaxed, rigor, and contracting muscle. *Biophys. J. 70* (4), 1836−1846.
(56) Ferenczi, M. A., Bershitsky, S. Y., Koubassova, N., Siththanandan, V., Helsby, W. I., Panine, P., Roessle, M., Narayanan, T., and Tsaturyan, A. K. (2005) The "roll and lock" mechanism of force generation in muscle. *Structure 13* (1), 131−141.
(57) Midde, K., Rich, R., Marandos, P., Fudala, R., Li, A., Gryczynski, I., and Borejdo, J. (2013) Orientation and Rotational Motion of Cross-

Bridges Containing Phosphorylated and de-Phosphorylated Myosin Regulatory Light Chain. *J. Biol. Chem. 288* (10), 7012−7023.
(58) Duggal, D., Nagwekar, J., Rich, R., Midde, K., Fudala, R., Gryczynski, I., and Borejdo, J. (2013) Phosphorylation of myosin regulatory light chain has minimal effect on kinetics and distribution of orientations of cross-bridges of rabbit skeletal muscle. *Am. J. Physiol. 306* (4), R222−R233.
(59) Gomes, A. V., and Potter, J. D. (2004) Molecular and cellular aspects of troponin cardiomyopathies. *Ann. N.Y. Acad. Sci. 1015*, 214−224.
(60) Colson, B. A., Locher, M. R., Bekyarova, T., Patel, J. R., Fitzsimons, D. P., Irving, T. C., and Moss, R. L. (2010) Differential roles of regulatory light chain and myosin binding protein-C phosphorylations in the modulation of cardiac force development. *J. Physiol. 588* (Part 6), 981−993.